Insights into the phosphoryltransfer mechanism of human thymidylate kinase gained from crystal structures of enzyme complexes along the reaction coordinate

Nils Ostermann[1], Ilme Schlichting[1], Ralf Brundiers[2], Manfred Konrad[2], Jochen Reinstein[1], Thomas Veit[1], Roger S Goody[1]* and Arnon Lavie[1†]

Background: Thymidylate kinase (TMPK) is a nucleoside monophosphate kinase that catalyzes the reversible phosphoryltransfer between ATP and TMP to yield ADP and TDP. In addition to its vital role in supplying precursors for DNA synthesis, human TMPK has an important medical role participating in the activation of a number of anti-HIV prodrugs.

Results: Crystal structures of human TMPK in complex with TMP and ADP, TMP and the ATP analog AppNHp, TMP with ADP and the phosphoryl analog AlF_3, TDP and ADP, and the bisubstrate analog TP_5A were determined. The conformations of the P-loop, the LID region, and the adenine-binding loop vary according to the nature of the complex. Substitution of ADP by AppNHp results in partial closure of the P-loop and the rotation of the TMP phosphate group to a catalytically unfavorable position, which rotates back in the AlF_3 complex to a position suitable for in-line attack. In the fully closed state observed in the TP_5A and the TDP–ADP complexes, Asp15 interacts strongly with the 3′-hydroxyl group of TMP.

Conclusions: The observed changes of nucleotide state and conformation and the corresponding protein structural changes are correlated with intermediates occurring along the reaction coordinate and show the sequence of events occurring during phosphate transfer. The low catalytic activity of human TMPK appears to be determined by structural changes required to achieve catalytic competence and it is suggested that a mechanism might exist to accelerate the activity.

Addresses: [1]Max Planck Institute for Molecular Physiology, Department of Physical Biochemistry, Otto-Hahn-Strasse 11, 44227 Dortmund, Germany and [2]Max Planck Institute for Biophysical Chemistry, Department of Molecular Genetics, 37018 Göttingen, Germany.

†Present address: University of Illinois at Chicago, Department of Biochemistry and Molecular Biology, 1819 W. Polk Street, Chicago, IL 60612, USA.

*Corresponding author.
E-mail: roger.goody@mpi-dortmund.mpg.de

Keywords: conformational change, crystal structures, P loop, thymidylate kinase

Received: **10 February 2000**
Revisions requested: **7 March 2000**
Revisions received: **22 March 2000**
Accepted: **23 March 2000**

Published: **30 May 2000**

Structure 2000, **8**:629–642

0969-2126/00/$ – see front matter

Introduction

Phosphoryltransfer reactions are among the most common reactions in biological systems and are catalyzed by ubiquitous enzymes that are generally referred to as kinases or phosphatases, or hydrolases if the acceptor is water. Typically, nucleotides are the phosphoryl donors of kinases. The range of phosphoryltransfer reactions catalyzed by these kinases includes such processes as the stepwise phosphorylation of nucleosides to nucleoside monophosphates (NMPs), then to nucleoside diphosphates (NDPs), and ultimately to nucleoside triphosphates (NTPs). The cascade of kinases that activate nucleosides to NTPs is of medical significance as it is responsible for the activation of antiviral prodrugs such as 3′-azido-3′-deoxythymidine (AZT) and 2′,3′-didehydro-2′,3′-dideoxythymidine (d4T). The conversion of these compounds from the monophosphate metabolite to the diphosphate is catalyzed by thymidylate kinase (EC 2.7.4.9, ATP:TMP phosphotransferase). Physiologically, thymidylate kinase (TMPK) catalyzes the reversible phosphorylation of thymidine monophosphate (TMP) using adenosine triphosphate (ATP) as its preferred phosphoryl donor [1] according to the following scheme:

$$TMP + ATP{*}Mg \rightleftharpoons TDP + ADP{*}Mg$$

In contrast to other nucleoside monophosphate kinases (NMPKs), TMPK is cell-cycle regulated with its expression limited to the S phase of cell replication [2,3]. The location of TMPK at the junction of the *de novo* and salvage pathways for thymidine triphosphate (TTP) synthesis makes this enzyme essential for DNA replication. Therefore, potent and selective inhibitors of human TMPK could have a role in cancer chemotherapy. A prerequisite for the rational design of such compounds is a detailed understanding of the catalytic machinery of TMPK at the molecular level.

Yeast and *Escherichia coli* TMPK are globular dimeric proteins with a similar fold to other NMPKs. Sequence homology and biochemical data, corroborated by the previously determined structures of yeast [4] and *E. coli* [5]

TMPK, demonstrate that three loops are crucial for the function of this enzyme. The first is the highly conserved P-loop motif [6] (consensus sequence $GX_1X_2X_3X_4GKS/T$, in single-letter amino acid code), which binds and positions the α- and β-phosphoryl groups of the phosphoryl donor (ATP) through interactions between amide backbone hydrogens and phosphate oxygen atoms. Unique to TMPKs is an interaction between the P-loop (residues 13–17 of human TMPK) and the phosphoryl acceptor (TMP) [4,5]. This is achieved through a hydrogen bond between the 3′-hydroxyl group of TMP and a carboxylic acid residue at position X_2 of the P-loop motif. The exact function of this residue is still unclear but it seems to be very important for the catalytic mechanism of TMPK as any mutation of this residue in either the yeast, human or *E. coli* enzyme abolishes activity [7].

The second critical loop contains the DR(Y/H) motif characteristic of TMPKs [8]. The aspartic acid residue (Asp96 in the human enzyme) is important for the binding and positioning of the magnesium ion complexed to ATP. The adjacent arginine residue (Arg97) acts as a clamp to bring the donor and acceptor nucleotides together by simultaneously making an interaction to the phosphate group of TMP and the γ-phosphate of ATP. The ϕ/ψ angles (80°/150°) of this arginine residue place it in the disallowed area of the Ramachandran plot (observed in all TMPK structures across three species). The function of this backbone strain is still unclear, but might be related to the catalytic importance of this residue. The third loop is the so-called LID region (residues 135–150). The LID is a flexible stretch that closes on the phosphoryl donor when it binds.

NMPKs bind the acceptor and donor nucleotides (the respective NMP as phosphoryl acceptor and in general ATP as the phosphoryl donor) such that the phosphate groups face each other. The kinetic mechanism of mouse TMPK and the homologous guanylate kinase (GMPK) and adenylate kinase (AMPK) has been shown to be random bi-bi in which the nucleotides bind independently of each other [9–11]. Crystal structures of substrate-free AMPK and AMPK in complex with only one substrate, both substrates or the bisubstrate inhibitor AP_5A showed that NMPKs undergo large conformational changes upon substrate binding [12]. One can distinguish between an open conformation without substrate, a partially closed conformation with a single substrate and a fully closed and active conformation in the presence of both substrates (or in the presence of AP_5A) [12]. In the fully closed structures of AMPK — and analogous structures of uridylate kinase (UMPK) — phosphoryl groups of both substrates interact with arginine sidechains of the LID region, revealing their importance in catalyzing phosphoryltransfer [13–15]. Eukaryotic TMPKs seem to work differently, however, as they possess no basic residues in the LID that could interact with the substrates.

To further our understanding of the catalytic mechanism of TMPK, we have extended the structural work to the human enzyme. We crystallized complexes of human TMPK that represent different states along the reaction coordinate. Here, we present the high-resolution structures of human TMPK in complex with TMP and ADP, TMP and the ATP analog AppNHp (β,γ-imidoadenosine 5′-triphosphate), TMP with ADP and the phosphoryl group mimic aluminum fluoride AlF_3, ADP and TDP, and TP_5A (a bisubstrate/biproduct inhibitor). Our data show the enzyme and nucleotides in different conformations. We correlate these changes with the different states that occur during the enzymatic reaction. This requires an extension of the minimal reaction scheme by at least two additional steps for human TMPK.

Results

Human TMPK consists of 212 amino acid residues with a calculated molecular weight of 24 kDa. It is a homodimeric globular protein (Figure 1a) with a similar fold to that described for the yeast and *E. coli* TMPKs [5,16]. Each monomer consists of a five-stranded parallel β-sheet core surrounded by nine α helices. The highly hydrophobic dimer interface is generated by the stacking of three nearly parallel helices from each monomer against each other. The determinants of substrate specificity are similar to those in yeast TMPK [4].

Substrate-induced conformational changes

In all structures presented here both nucleotide-binding sites are occupied, resulting in globally closed conformations of the enzyme. A novel feature observed in the human TMPK structures concerns the additional conformational changes that occur within this globally closed conformation, which are dependent on the nature of the bound substrates. This newly recognized feature entails the rigid-body movement of three loop regions — the P-loop (residues 13–17), the LID (residues 135–150), and the adenine-base binding loop (residues 178–188). Thus, within the globally closed conformation we observe different conformations for these regions (Figure 1b). The first conformation, which we term 'P-loop open', is formed in the presence of TMP and ADP. The second, the 'P-loop partially closed' conformation, results when ADP is replaced by AppNHp or when AlF_3 is soaked into a TMP–ADP crystal (1.1 Å movement measured at the Cα atom of Asp15). The third state, the 'P-loop closed' conformation, is occupied when TP_5A is present (2.1 Å movement measured at the Cα atom of Asp15 compared with the open conformation) or in the presence of the products TDP and ADP. Although with each P-loop movement a concomitant shift in the position of the LID region and the adenine-base binding loop is also observed, we choose the above terminology that focuses on the P-loop, because of the importance of this loop and for clarity. It should be kept in mind, however, that all three loops undergo

Figure 1

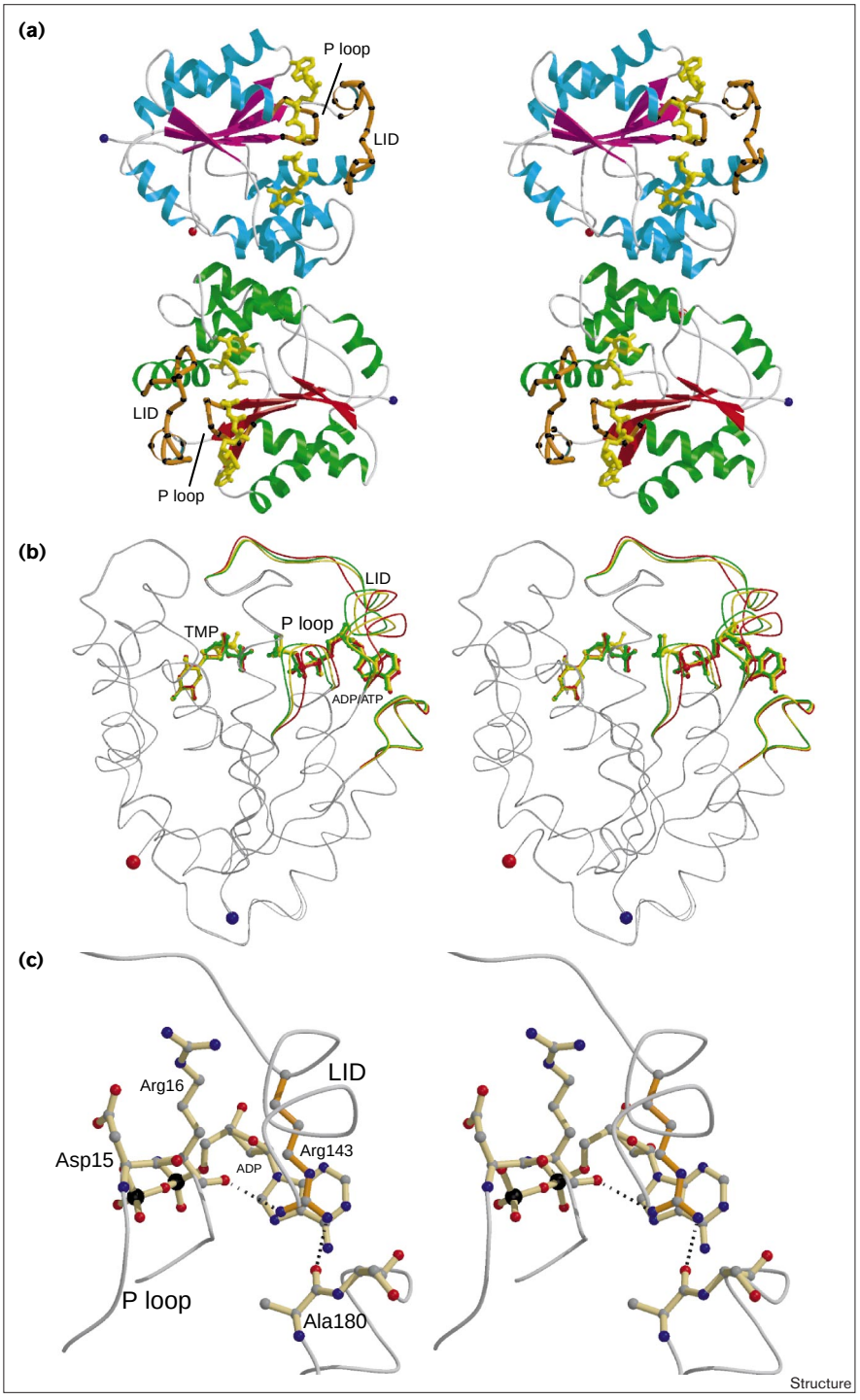

Rigid-body movements within the substrate-bound, globally closed conformation of the homodimeric human TMPK in response to the nature of the bound substrates. **(a)** Stereoview ribbon diagram of the globally closed conformation of the TMPK dimer in complex with TMP and AppNHp (substrates in yellow; α helices in green or cyan, and β strands in red or magenta to differentiate between monomers). Loops are depicted as gray coils, except for the P-loop and LID regions which are colored orange with black Cα atoms. **(b)** Stereoview overlay of three TMPK monomers to illustrate the different conformations within the globally closed conformation (root mean square deviation [rmsd] for all Cα atoms except the colored regions < 0.17 Å). The three regions that undergo conformational changes – the P-loop, LID and adenine base binding loop – are colored. Within the globally closed conformation we differentiate between an open conformation that is formed when TMP and ADP are bound (red), the partially closed conformation in the presence of TMP and AppNHp (yellow) and the fully closed state when TP_5A is bound (green). **(c)** Stereoview close-up of the colored regions of (b) (same orientation). Arg143 (orange) from the LID region has a crucial role in the communication between the regions that are involved in the rigid-body movement. Arg143 forms a base-stacking interaction with the adenine base and hydrogen bonds to backbone carbonyl oxygens of Arg16 of the P-loop and Ala180 of the adenine base binding loop. The figures were generated using the programs Molscript [28] and Raster3D [29].

conformational changes upon transition between the different states. The P-loop moves as a rigid body, with the hinges being formed by two highly conserved residues: Glu12, which anchors the P-loop via a bidentate interaction with the hydroxyl (2.5 Å) and the amide (2.9 Å) groups of Ser101, and Lys19, which interacts with the phosphate(s).

These conformational changes are not observed in other structurally characterized NMPKs and seem to be unique to TMPK. In the case of AMPK no P-loop conformational change is observed between the complexes with AMP and ADP (Protein Data Bank [PDB] accession code 2eck) and with AMP and AppNHp [17]. Likewise, structural

comparisons of UMPK in complex with UMP and ADP in the presence or absence of the transition-state analog AlF_3 shows no P-loop mainchain atom movement [15]. To the best of our knowledge, no P-loop movement in GTP- or ATP-binding proteins has been observed upon replacement of a diphosphate by a triphosphate.

As in other NMPKs, an arginine from the LID region (Arg143) forms a stacking interaction with the adenine base. The guanidinium group of this arginine also interacts with the mainchain carbonyl oxygens of both Arg16 of the P-loop (3.1 Å) and Ala180 (2.7 Å) of the third region involved in the rigid-body movement (see above and Figure 1c). Thus Arg143 seems to have a crucial role for the communication between the base of the phosphoryl donor and the three regions observed in different conformations within the globally closed conformation.

The complex with TMP and ADP

The structure of human TMPK in complex with TMP and ADP shows the P-loop open conformation (Figure 2a). The hydrogen-bonding network built by seven water molecules located between the P-loop and the monophosphate seems to be crucial in stabilizing this conformation. The 3′-hydroxyl of the TMP ribose interacts with water molecule Wat510, which makes further interactions to other waters (Wat512 and Wat790) that for their part interact with protein residues (Arg97 and Gln157) and additional water molecules. Wat512 connects Wat510 and Wat508, the latter and Wat507 (which is coordinated to Mg^{2+}) acting as 'space fillers' for the γ-phosphoryl group in ATP. Further strongly bound water molecules (511, 513 and 514 with very good electron density and low B factors) are placed between the P-loop and TMP such that they form hydrogen bonds to both the P-loop and the sidechain of Arg97, a residue that is involved in TMP binding. In the P-loop open conformation the distance between the sidechain of Asp15 and the 3′-hydroxyl of TMP is 6.8 Å. This is noteworthy because in the 'P-loop closed' conformation this aspartate interacts with the 3′-hydroxyl group (see below). As many nucleoside analogs with antiviral activity are modified at this position (e.g., the azido group of AZT replaces the 3′-hydroxyl of TMP), the interactions made by a 3′-substituent and the enzyme are likely to be critical for the ability of the enzyme to phosphorylate the analog. The TMP phosphoryl group is positioned by two hydrogen bonds between OP2 and OP1 to Arg97 (2.7 Å and 2.9 Å to atoms NE and NH2, respectively), and a water-mediated interaction (Wat509) between OP3 and NH2 of Arg45 (2.2 Å and 2.7 Å, respectively). In addition, each of the phosphate oxygen atoms interacts with a water molecule that coordinates the ADP-bound magnesium ion (distances between 2.7 Å and 2.9 Å).

The complex with TMP and AppNHp

As the complex with TMP and AppNHp crystallizes isomorphously with the TMP and ADP complex, we used the coordinates of the latter to start refinement. Upon inspection of the resulting electron-density map we observed density at the expected position of a γ-phosphate. However, the electron-density for the P-loop and LID region was of inferior quality. Further refinement with extensive use of omit maps revealed that the P-loop and LID regions have two conformations: one previously seen in the ADP complex, and an additional conformation termed 'P-loop partially closed' (maximum backbone movements of 1.4 Å and 2.3 Å Cα for the atoms of Val14 [P-loop] and Leu137 [LID], respectively). Therefore, the electron density was interpreted as representing two states: the first, with an occupancy of one-third, has ADP present at the phosphoryl donor site and the P-loop and LID in the open conformation, a conformation identical to that described above for the TMP–ADP complex. The second state, with an occupancy of two-thirds, has AppNHp at the phosphoryl donor binding site and the P-loop and LID in the partially closed conformation (Figure 2b). The observation of both ADP and AppNHp in the complex is probably a result of using an ADP-bound enzyme preparation for the crystallization setups. Despite following a purification protocol in which no nucleotides were present, the pure TMPK contains approximately 20% TMP and ADP. Attempts to obtain nucleotide-free enzyme were not successful. To increase the occupancy of AppNHp, the crystallization setups contained 20 mM of the ATP analog. An alternative reason for the ADP observed might be the hydrolysis of AppNHp during the crystallization procedure. In this case, ADP–NH_2, which would be indistinguishable from ADP, would be bound. The presence of two states is consistent with high B factors for the γ-phosphate of AppNHp if modeled with an occupancy of one, and its relatively weak density. Concomitant with the P-loop and LID, the region between residues Ala180 and Val187 (maximal movement at Cα of Lys182 is 0.3 Å) and AppNHp with its bound magnesium ion move towards the monophosphate (0.2 Å). Although the magnitude of this movement is close to the coordinate error, the displacement seems to be significant as it includes a whole region and not only a few uncorrelated atoms.

In addition to the mixture of ADP and AppNHp, we observe the phosphoryl group of TMP in two conformations (but with a single conformation for the base and ribose moieties). In one conformation, the phosphoryl group is in the same position as in the complex with TMP and ADP and is modeled with an occupancy of one-third. The other conformation, modeled with an occupancy of two-thirds, has the phosphate group displaced (2.2 Å between the phosphate atoms of the two states) and correlates with AppNHp binding. Thus, in the presence of AppNHp, the phosphoryl group of TMP does not interact with Arg97, but rather forms a hydrogen bond (2.7 Å) with NH2 of Arg45. The high-resolution and quality of our data enables us to observe and estimate the partially occupied states quite accurately.

Figure 2

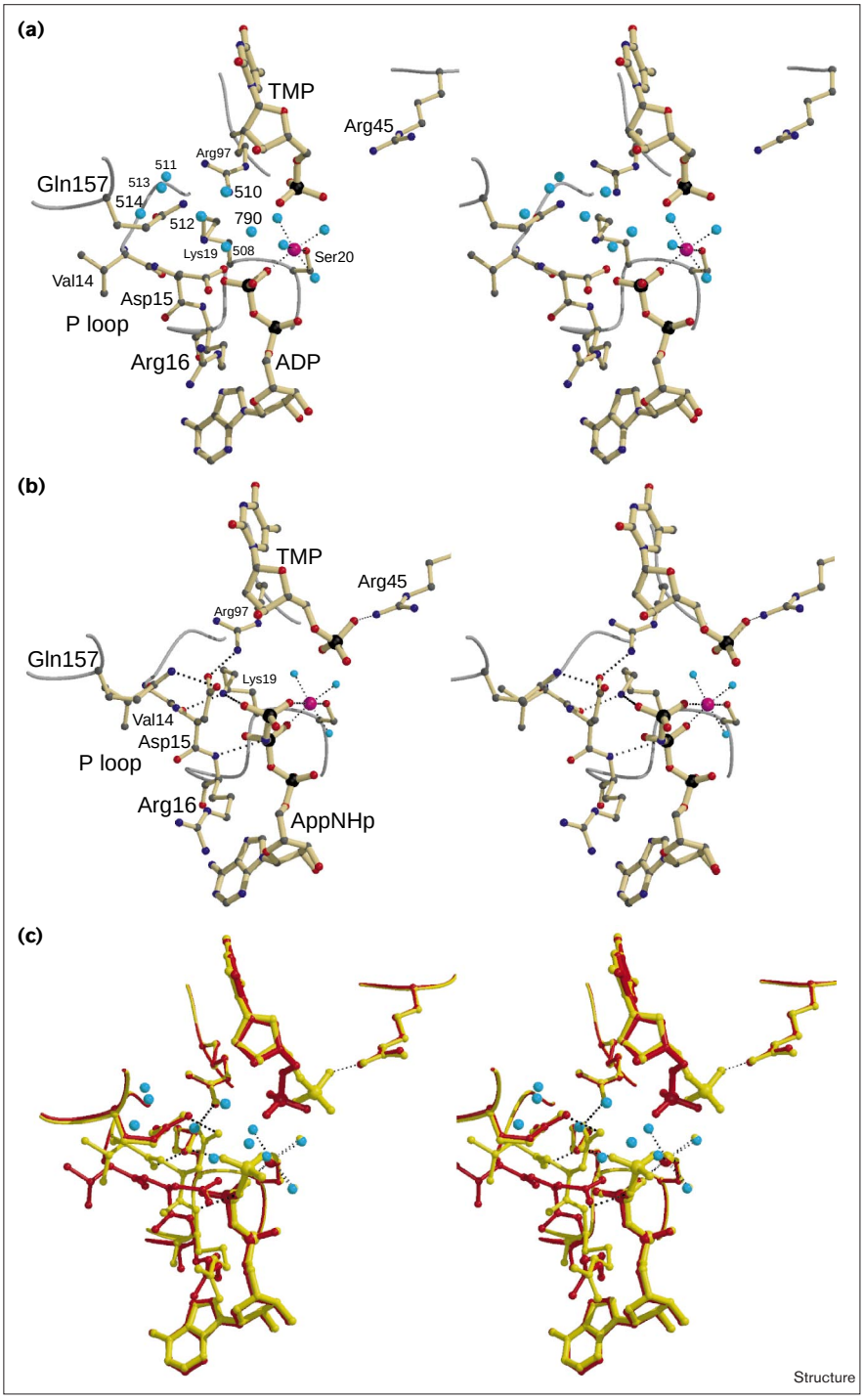

Comparison of the open and partially closed active-site conformations of human TMPK reveal the reasons for the P-loop closure upon replacement of ADP by AppNHp. Nucleotides and selected protein residues are shown in a ball-and-stick representation, the magnesium ion (magenta) is connected with thin dashed lines to its six ligands. **(a)** Stereoview of the open P-loop conformation of TMPK in complex with TMP and ADP. The seven water molecules (numbered cyan spheres) located between the P-loop and TMP build a hydrogen-bonding network that stabilizes the open P-loop conformation. **(b)** Stereoview of the partially closed P-loop conformation of TMPK in complex with TMP and AppNHp. New interactions (shown as thick dashed lines) that are not possible in the open conformation stabilize this conformation. **(c)** Stereoview overlay of (a) (red) and (b) (yellow) shows that the γ-phosphoryl group of AppNHp displaces two water molecules (507 and 508) and induces the sidechain of Asp15 to rotate towards the 3′-hydroxyl of TMP. The rotation of Asp15 results in the displacement of water molecules 510, 512 and 790. Thus, the binding of the γ-phosphoryl group in AppNHp results in the destabilization of the open conformation as it induces the replacement of at least five water molecules that are involved in the stabilization of the open P-loop conformation. Concomitantly, the partially closed conformation is stabilized by interactions that are not possible in the open conformation. The figures were generated using the programs Molscript [28] and Raster 3D [29].

The γ-phosphoryl group of AppNHp interacts with both Arg97 NH2 (3.2 Å) and Lys19 NZ (2.8 Å) through the oxygen atom O3P (Figure 2b). In addition to these interactions, the P-loop partially closed conformation is stabilized by many new interactions that are not observed in the P-loop open conformation. These include hydrogen bonds between several pairs of residues: the sidechain of Asp15 and NH2 of Arg97 (2.7 Å); the sidechain of Asp15 and Gln157 (2.9 Å); the amino group of the highly conserved Lys19 and the backbone carbonyl of Val14 of the P-loop (2.6 Å compared to 3.6 Å in the open conformation); and the amide of Arg16 and the imido group between the

β- and γ-phosphates of AppNHp (3.1 Å versus 3.4 Å in the open conformation). Whereas in the open conformation the P-loop and LID interact directly (3.2 Å) via the amide of Val14 and the carbonyl group of Leu133, this interaction is broken in the partially closed state, where a water molecule (Wat511) bridges the two regions.

The TMP–ADP–AlF_3 complex

The P-loop partially closed conformation is also observed in the presence of the phosphoryl group mimic AlF_3 (see Supplementary material), which is expected to simulate the transition-state conformation based on earlier work mainly on GTPases and ATPases (for a review see [18]). In the TMP–ADP–AlF_3 complex the distance between OP5 of ADP — the leaving group atom during the phosphoryltransfer reaction — and the amide nitrogen of the Arg16 of the P-loop is 2.9 Å. The TMP phosphoryl group is in a position between that seen in the TMP–ADP- and the TMP-AppNHp-bound states (Figure 3a). The phosphoryl group of TMP is placed such that the OP3 oxygen atom makes a 2.9 Å interaction to NE of Arg97, and OP2 is at a distance of 3.5 Å from NH2 of Arg45. Importantly, the TMP phosphate oxygen that points toward the AlF_3 molecule makes no interaction with the enzyme and seems to be in an optimal position for nucleophilic attack. Precise modeling of AlF_3 is difficult due to the ambiguous electron density, consistent with the very weak affinity (see Materials and methods). In the last step of the refinement, we modeled the remaining positive F_o–F_c difference electron density as AlF_3, which is in line with other structures determined at pH 8.0 [19].

The complex with TDP and ADP

Because this complex was crystallized in the presence of both substrates, a mixture of substrates and products would be expected. However, at the phosphoryl donor site we do not observe any density that would correspond to the γ-phosphate of ATP (ADP is therefore modeled with an occupancy of one, and at the acceptor site, we observe predominately TDP (modeled with two-thirds occupancy, one-third is modeled as TMP). In this complex the P-loop and LID are in the fully closed conformation (maximal shift of the P-loop between the open and closed conformation is 2.1 Å at the Cα atom of Asp15). Concomitant with the P-loop and LID region, ADP with its associated magnesium ion shifts by 0.5 Å in the direction of TDP, so that the distance between the leaving oxygen atom of ADP and amide nitrogen of Arg16 remains at 2.9 Å. The carboxylate group of Asp15 rotates by 30° compared with its position in the complex with either TMP–AppNHp or TMP–ADP–AlF_3, and is in a position to make a bidentate interaction with the 3′-hydroxyl of TDP. The most pronounced conformational changes in this complex, in comparison to the structures described above, are a 90° rotation of the Arg97 sidechain around the bond between atoms CG and CD, and a rearrangement of the TDP phosphates (Figure 4). In the TDP–ADP-bound conformation, NE of Arg97 hydrogen bonds to the carbonyl oxygen of Phe42. The carbonyl group of Phe42 is fixed at this position as the following amino acid is a highly conserved *cis*-proline. This interaction may explain why this residue adopts the *cis* conformation. At the same time, the phosphoryl groups of TDP rearrange with a 3.8 Å shift of the α-phosphate of TDP in comparison to the phosphate position of TMP in the AlF_3 complex. The new position of the phosphates is fixed by interactions between the α-phosphate and Arg45 and two hydrogen bonds between OP3 and OP4 of the β-phosphate and NH1 and NH2 of Arg97 (2.9 Å and 2.8 Å, respectively). At the position of Arg97 as seen in the other complexes, there are two water molecules (Wat515 and Wat516) that act as space fillers for the arginine sidechain in the product-bound complex. These water molecules form hydrogen bonds to the P-loop, thereby stabilizing this conformation.

Complex with TP_5A

The fully closed protein conformation observed in the TP_5A complex is similar to the protein conformation when TDP and ADP are bound. However, Arg97 is not in the rotated conformation but remains in the position seen in the AppNHp and AlF_3 structures, due to the covalently linked phosphate chain of the nucleotide analog that prevents such a rotation. In this conformation the distance between OD1 of Asp15 and NH2 of Arg97 is 2.2 Å, and the distance between OD1 of Asp15 and O2G of the middle phosphoryl group of TP_5A is 3.0 Å. The O2G of TP_5A interacts with basic residues that may shield the negative charge (3.0 Å and 2.9 Å to Lys19 NZ and Arg97 NH_2, respectively).

Despite the lack of electron density for the additional phosphoryl group — the one bridging TMP and ATP in TP_5A — and despite only poor density for the middle phosphoryl group of TP_5A, the presence of TP_5A in the crystals was established for the following reasons. First, we observe the fully closed conformation of TMPK (in the presence of TMP and ADP we observe the open conformation). Second, we determined the K_d of the complex of TP_5A and human TMPK to be 210 ± 30 nM, allowing the formation of a stoichiometric complex under the crystallization conditions (concentrations of TMPK and TP_5A were 1 mM and 2 mM, respectively). Third, high pressure liquid chromatography (HPLC) analysis of dissolved crystals unambiguously demonstrated the presence of TP_5A.

Discussion

NMPKs are highly flexible molecules that undergo large conformational changes upon substrate binding [12]. In the presence of both nucleotides, these enzymes occupy a closed conformation. The structures of the surface mutant Arg200→Ala of human TMPK presented herein (the Arg200→Ala mutant has identical kinetic and structural properties to wild-type TMPK, see the Materials and methods section) show that this kinase makes additional

Figure 3

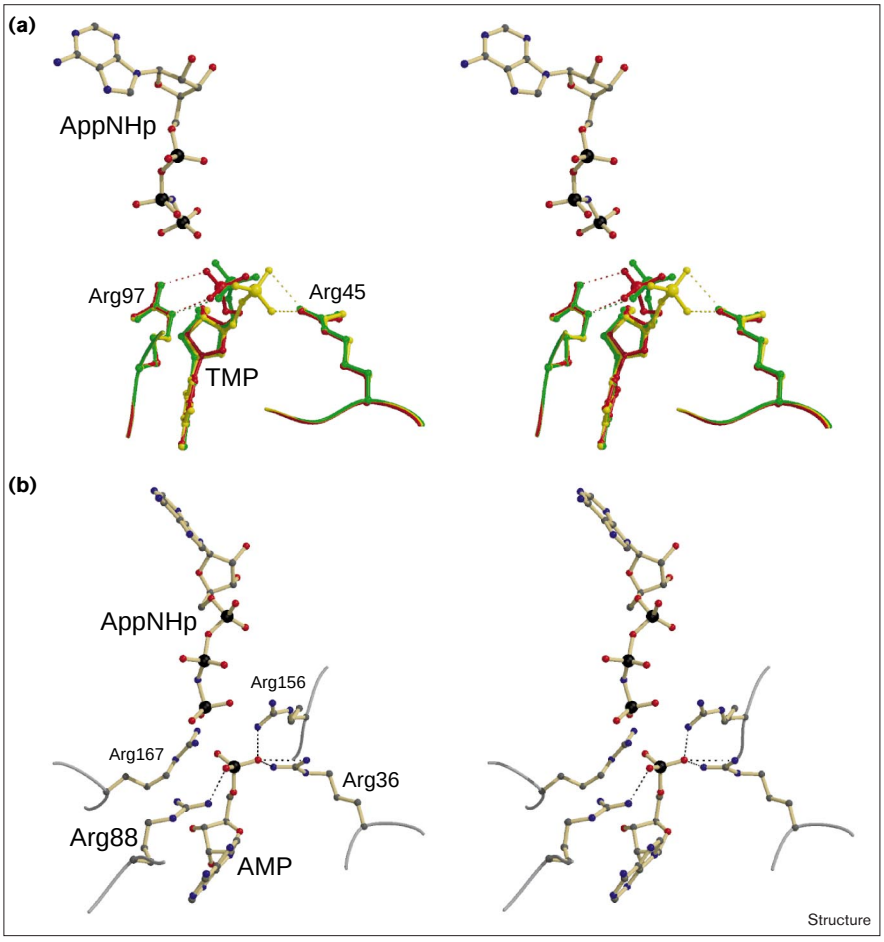

The different ways of positioning the phosphoryl groups of TMP and AMP by TMPK and AMPK, respectively, reveal the reasons for unique movements of the TMP phosphoryl group in the different TMPK complexes. **(a)** Stereoview overlay of TMP, Arg97 and Arg45 of the complexes of TMPK with TMP and ADP (red), TMP and AppNHp (yellow) and TMP with ADP and AlF_3 (green). AppNHp is shown to give the orientation for the nucleophilic attack of the monophosphate. It is only in the AlF_3 structure that the TMP phosphoryl group is in an optimal position for nucleophilic attack on the phosphoryl group to be transferred. **(b)** Stereoview positioning of the AMP phosphoryl group of AMPK in complex with AMP and AppNHp. In contrast to TMPK the AMP phosphoryl group is fixed in an optimal position for the nucleophilic attack by two additional arginine residues that are not present in TMPK. Two of the three oxygen atoms of the AMP phosphoryl group are hydrogen bonded to Arg88 and Arg36 (homologous to Arg97 and Arg45 in TMPK). In addition, Arg156 from the LID region makes an interaction to one oxygen atom of the AMP phosphoryl group and Arg167 is 3.6 Å from the attacking oxygen, leaving it free for the nucleophilic attack. The figures were generated using the programs Molscript [28] and Raster 3D [29].

conformational changes within a globally closed conformation that are dependent on the nature of the bound nucleotides. At this stage we cannot be sure whether this novel feature is unique to the human enzyme, or if it is a general feature of all TMPKs. In the following discussion the forward reaction (i.e., the production of ADP and TDP from ATP and TMP) will be considered, but it should be kept in mind that the overall reaction is reversible with an equilibrium constant near to unity.

The γ-phosphoryl group of AppNHp induces P-loop closure

The structure of TMPK in complex with TMP and ADP (a combination of substrate and product) shows an open conformation of the P-loop, the LID, and the adenine-binding region. Upon binding of the ATP analog AppNHp these three regions undergo concerted rigid-body movements, with the communication between the regions occurring mainly through Arg143. This residue is located in the LID region (Figure 1c) and forms a base-stacking interaction with the adenine base and hydrogen bonds to the backbone carbonyl oxygen atoms of Arg16 in the P-loop and Ala180 in the adenine-binding region.

The open P-loop conformation appears to be stabilized by a hydrogen-bonded network of water molecules that are located between the P-loop, Gln157 and TMP. Replacement of ADP by AppNHp induces a conformational change to a partially closed P-loop conformation (Figure 2c), which can be rationalized by the following scenario. Upon binding, the γ-phosphoryl group of AppNHp displaces Wat507, which is coordinated to the magnesium ion when ADP is bound, and Wat508. Thus, these water molecules function as space fillers for the γ-phosphoryl group in the TMP–ADP complex. In addition, the presence of the γ-phosphoryl group of AppNHp causes the sidechain of Asp15 to rotate towards the 3′-hydroxyl group of the TMP ribose, but without approaching closely enough for an interaction to occur. The change in the Asp15 sidechain position results in the displacement of five more water molecules (510, 512, 513, 514 and 790), two of which (510 and 512) function as space fillers for the new Asp15 conformation. In this orientation, Asp15 interacts directly (and not via Wat514) with the sidechain carbonyl oxygen of Asn157, and the guanidinium group of Arg97. These interactions are made possible by the movement of

Figure 4

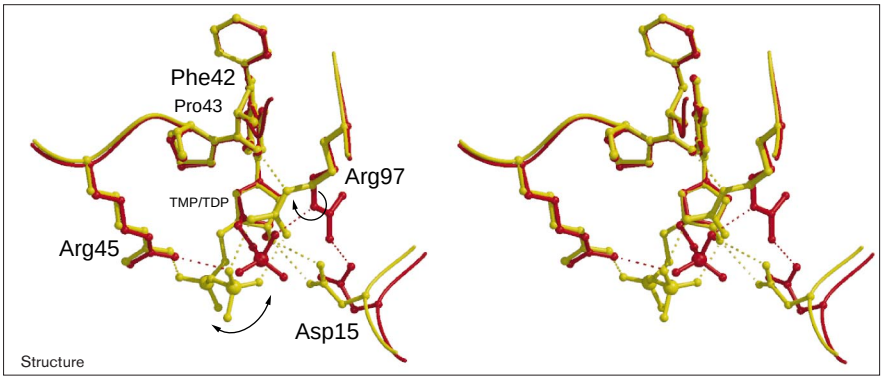

Conformational changes of Arg97 and the phosphoryl groups of TDP to the stable product conformation in the TDP–ADP bound complex. Overlay of the TMP/TDP-binding site of the structures of TMPK in complex with TMP, ADP and AlF_3 (red) and TDP and ADP (yellow). In the complex with bound TDP and ADP the sidechain of Arg97 rotates (90°) around the bond between the atoms CG and CD such that it cannot act as a clamp to bring both nucleotides together for the backward reaction. The figures were generated using the programs Molscript [28] and Raster 3D [29].

the P-loop to the P-loop partially closed conformation. Therefore, the shift from the open P-loop conformation to the P-loop partially closed conformation is a consequence of the break in the water structure that stabilizes the open conformation and of the formation of new interactions only possible in the partially closed conformation.

Any valid mechanistic interpretation of the structure with AppNHp bound is dependent on it being a good ATP analog for TMPK. In the TMP–AppNHp complex, the lone electron pair of the bridging imido group between the β- and γ-phosphoryl group interacts (distance 3.1 Å) with the amide of Arg16 located in the P-loop. An analogous interaction is seen in all P-loop-containing enzymes the structures of which have been determined in the triphosphate-bound state. This interaction is important for stabilizing the negative charge that arises at the leaving oxygen atom (the atom that bridges the β- and γ-phosphates) during the phosphoryltransfer reaction. Therefore, a correlation between the chemical nature of the bridging group and the P-loop conformation is of great mechanistic importance (see below). The recent analysis of $p21^{ras}$ complexed with GppNHp or with GTP shows no significant difference between the two structures either in the P-loop conformation or the nucleotide position [20]. This detailed analysis led to the conclusion that in the case of $p21^{ras}$, GppNHp is a good GTP analog. However, AppNHp is not a good analog of ATP in all systems. The best documented example is myosin ATPase, where it has been shown that AppNHp binds many orders of magnitude more weakly than ATP and is only able to mimic some of the consequences of ATP binding in physiological and biochemical experiments. This appears to be due to the fact that, in this system, correct binding of ATP requires not only a P-loop backbone interaction with the bridging β,γ-oxygen but also an interaction of this oxygen with an asparagine sidechain [21]. This is not possible with AppNHp. If such an interaction were important for TMPK, it might be expected to be seen in the AlF_3 complex, which is not the case. In addition, the affinity of TMPK for AppNHp, although lower than for ATP, is only reduced by a factor of 30 (NO *et al.*, unpublished results), similar to the situation for $p21^{ras}$. On the basis of these considerations, we conclude that AppNHp is a valid ATP analog in the case of TMPK, and that the observed P-loop partially closed conformation is mechanistically important.

We designate the P-loop partially closed conformation as an active conformation in the sense that it is structurally close to the active ground state of the forward reaction (defined here as the state immediately preceding attack of the phosphate of TMP on the β-phosphate of ATP) for the following reasons. First, P-loop closure is only observed in complexes with nucleotides that allow the aforementioned interaction between the β- and γ-phosphate bridging atom and the P-loop. (In the structure of TMPK in complex with $AppCH_2p$ the P-loop is in the open conformation; NO *et al.*, unpublished results). In complexes of human TMPK with AppNHp and the substrate TMP, the P-loop is partially closed whereas it is fully closed upon replacement of TMP by the substrate analog 3′-amino-3′-deoxythymidine monophosphate (NO *et al.*, unpublished results). Thus, the AppNHp imido group does not prevent P-loop closure, which strongly suggests that the P-loop partially closed conformation is mechanistically important. Second, in the AlF_3 complex, a state that could be interpreted to mimic aspects of the transition-state conformation, the P-loop is also in the partially closed conformation. Third, a correlation has been established between the ability of the enzyme to adopt the P-loop partially closed conformation and the *in vitro* steady-state phosphorylation rate with different TMP analogs (NO *et al.*, unpublished results). Fourth, the critical distance between the amide of Arg16 and the atom corresponding to the bridging atom between the β- and γ-phosphoryl groups in ATP (2.9 Å in AlF_3, 3.1 Å in AppNHp and 3.4 Å in ADP) shortens. Fifth, in the P-loop partially closed conformation, the carboxylic sidechain of the P-loop Asp15 interacts with the sidechains of the highly conserved Gln157

and Arg97. The latter interaction may have an important role in positioning this catalytic arginine and may also prevent an interaction with the attacking oxygen atom of the TMP phosphate group (as observed in the P-loop open state) by neutralizing its charge.

AlF_3 brings both TMPK and the substrates into an active conformation

Despite strong electron density for the AlF_3 moiety between the nucleotides, the density is not well defined, making the precise modeling of this group difficult. Therefore, it is not clear whether the quaternary complex of TMPK with TMP, ADP and AlF_3 reflects the structure of the transition state of the reaction, the Michaelis complex, or an activated ground state. It is highly probable, however, that of all the states described, it is closest in structure to the transition state.

The complex of TMPK with TMP, ADP and AlF_3 is interpreted as representing not only the active enzyme conformation (partially closed P-loop) but also the active conformation of the nucleotides. An overlay with the other structures shows that the protein structure is nearly identical to that seen in the complex with TMP and AppNHp. The P-loop moves slightly further towards the monophosphate, but all interactions are the same. Analysis of the different positions observed for the phosphate group of TMP in the structures presented here indicates that only in the AlF_3-bound state does the phosphoryl group adopt what appears to be an optimal position for a nucleophilic attack on the phosphoryl group to be transferred (simulated by AlF_3 in this case; Figure 3a). In the AlF_3 complex, the phosphate group of TMP makes only one interaction with Arg97, leaving the attacking oxygen atom free for nucleophilic attack on the γ-phosphate of ATP. In contrast, this phosphate oxygen atom forms a double interaction with Arg97 in the TMP–ADP-bound conformation, so that the negative charge would be partially shielded, making it a weaker nucleophile. Likewise, the TMP phosphate conformation observed in the TMP–AppNHp complex is not favorable for catalysis as the distance between the attacking oxygen and the phosphorous atom of the phosphoryl group to be transferred is longer than that seen in the AlF_3 conformation. We attribute this observation to the repulsion between the negatively charged oxygen atoms in TMP and the γ-phosphoryl group of AppNHp. Therefore, we only regard the TMP conformation in the AlF_3 complex as the active conformation for this nucleotide.

The TDP–ADP product complex

Crystallization of TMPK in the presence of the substrates TMP and ATP results in a fully closed conformation of the protein complexed with the products TDP and ADP, which are, of course, the substrates for the reverse reaction. Questions that must be asked at this point are why only the product complex is seen in the structure and whether this complex is on the normal catalytic pathway. Concerning the lack of electron density corresponding to the substrates, one must consider the following. The equilibrium constant for phosphate transfer is approximately unity in solution and presumably similar in the protein. A relatively small departure (in energetic terms) from this value in the direction of product formation could lead to a situation in which a minor population of the substrate complex would not be detected in the crystal structure. The departure from the value of the equilibrium constant for the free nucleotides in solution is therefore interpreted as the effect of the active site of the enzyme, perhaps combined with some effect of crystal packing forces. For the sake of present arguments, we assume that the observed conformation is on the reaction pathway. In the forward direction we interpret it to represent a state after phosphate transfer and before product release. The law of microscopic reversibility requires that the reaction pathway traversed in the forward reaction is also taken in the reverse direction, under identical conditions. Thus, if the structure of the complex with AlF_3 is considered to represent, or at least to approach, the transition-state structure for the forward reaction, it must serve the same function for the back reaction. (This interpretation is based on the assumption that the mechanism does not involve a discrete covalent intermediate; in such a case, two transition states are expected.) The product conformation we observe is very different from the conformation of the presumed transition-state complex analog seen with AlF_3, implying that a conformational change takes place after the chemical step (Figure 4). This means, in turn, that the structure we have characterized cannot be regarded as being the state immediately preceding attack of the β-phosphate of ADP on the β-phosphate of TDP in the back reaction. In keeping with this, the conformation observed appears to lack vital interactions required for catalysis because of a rotation of the diphosphate moiety of TDP with respect to the phosphate position when TMP is bound. As a result, the β-phosphoryl group of TDP (the transferred phosphoryl group) does not interact with the catalytic magnesium ion, but rather forms two hydrogen bonds to Arg97, which rotate concomitantly to a position very close to that previously occupied by the phosphate group of TMP. In the new position Arg97 cannot act as a clamp to bring the nucleotides together (as seen in the AlF_3 complex). Wat515 and Wat516 bind at the 'old' positions of the NH1 and NH2 atoms of Arg97, respectively, thereby preserving the Arg97 interactions (e.g., with the hydroxyl group of Ser101 or with the Asp15 carboxyl oxygen atom). The other carboxyl oxygen atom of Asp15 interacts with the 3′-hydroxyl of the TMP ribose and the amino group of the Gln157 sidechain.

The TMPK–TP_5A complex resembles the active enzyme–product conformation

Phosphate-linked dinucleotide inhibitors such as AP_5A, UP_5A or TP_5A have been extensively utilized in studies of NMPKs as transition state, bisubstrate or biproduct

Figure 5

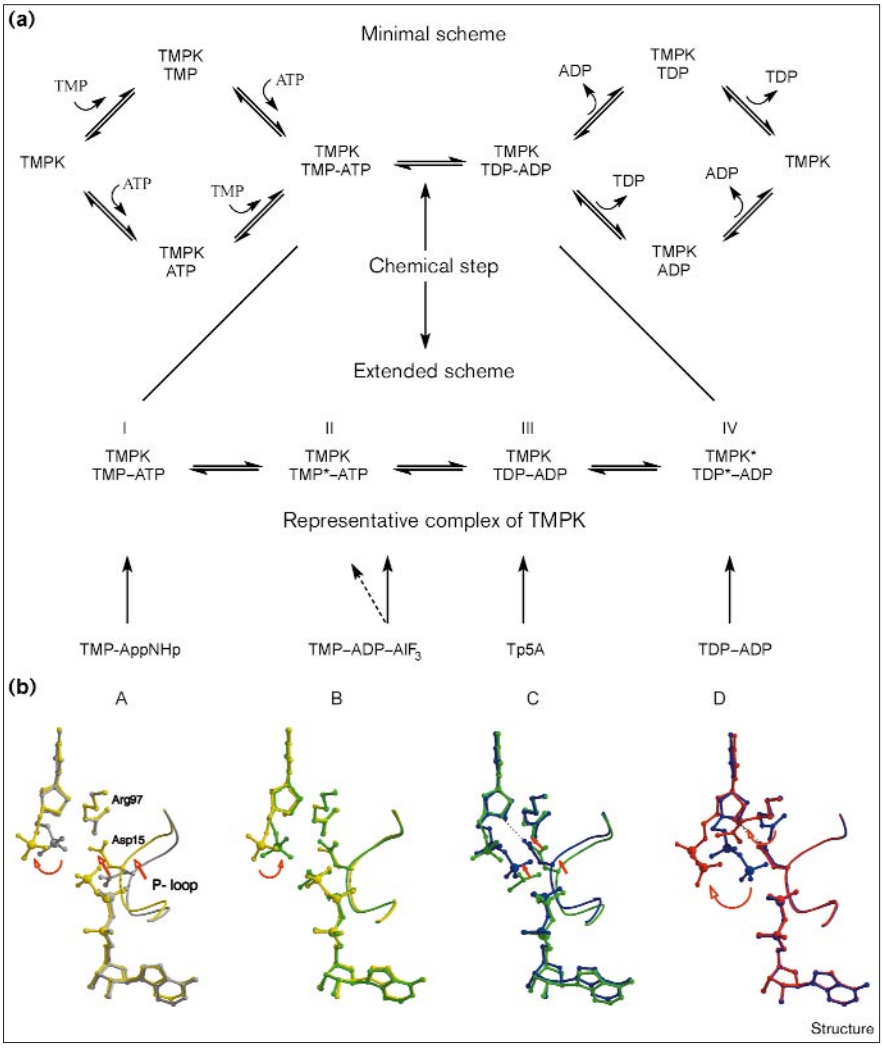

(a) The minimal scheme for a bi-bi mechanism requires an expansion to account for the conformational changes that occur after both substrates are bound and prior to product release. We have proposed these states, I, II, III and IV, on the basis of the different structural features observed in the different complexes of human TMPK **(b)**, labeled A, B, C and D: (A) overlay of the TMP–ADP (gray) and TMP–AppNHp (yellow) complexes; (B) TMP–AppNHp and TMP–ADP–AlF_3 (green); (C) TMP–ADP–AlF_3 and Tp5A (blue; the β-phosphate group of Tp5A is modeled; (D) Tp5A and TDP–ADP (red). Superposition of the different states reveals the possible dynamics that occur during the phosphoryltransfer reaction. Note that the TMP–ADP complex shown in (A) does not represent a state on the reaction coordinate, but rather reveals the conformational changes that occur upon the replacement of a diphosphate by a triphosphate at the phosphoryl donor site.

mimics [5,14,16,22]. A complex of AMPK and AP_5A was interpreted to simulate the substrate-bound conformation [23], whereas for UMPK the analogous complex with UP_5A was interpreted as representing the product-bound conformation rather than the substrate-bound state [14]. The overlay of the human TMPK–TP_5A structure with the other structures shows that the protein conformation is nearly identical to that seen in the TDP–ADP complex (interpreted as an isomerized product complex). The only difference in protein structure between the complexes is the orientation of the Arg97 sidechain. This residue adopts the same conformation as in the ADP, AppNHp or AlF_3 complex and interacts with the γ-phosphate of the ATP moiety of TP_5A. The interaction between the P-loop carboxylic acid and the 3′-hydroxyl of TDP in the TDP–ADP complex structure, or to the corresponding atom in the presence of TP_5A, is nearly identical and quite different from that seen in the other structures. There is no electron density for the phosphate group linking the ATP and TMP moiety in TP_5A, and the temperature factors for the terminal phosphates of ATP and TMP are high. Therefore, and because of the high similarity in the protein structures of the TDP–ADP and TP_5A complexes, we interpret the TP_5A-bound complex as the enzyme conformation immediately after the phosphoryltransfer but prior to the conformational change to the product conformation discussed above.

What is the role of Arg16?

The P-loop of all eukaryotic TMPKs contains an arginine residue that follows the strictly conserved carboxylic acid. In the yeast TMPK–TP_5A complex, an interaction between the sidechain of Arg15 and the middle phosphate group of the inhibitor was observed. Taken together with the result that mutating this arginine to glycine in the yeast enzyme reduces the activity 200-fold [7], we

assigned a catalytic role to this residue [16]. In all of the human TMPK complex structures, however, we observe this arginine in an extended conformation that precludes interaction with the phosphates. This result is consistent with mutagenesis experiments that show no appreciable decrease in catalytic rate upon mutating this residue to glycine [7]. Interestingly, the rate observed for the human enzyme (0.7 sec^{-1}) is similar to that measured for the yeast enzyme lacking this residue (35 sec^{-1} for wild type, 0.2 sec^{-1} for the Arg15→Gly mutant [7]). Thus, a critical difference between the yeast and the human enzymes (44% sequence identity) seems to be the role of the P-loop arginine, which seems to be catalytically important only in the yeast enzyme. It should be pointed out, however, that this interpretation is not conclusive, as there is as yet no available evidence concerning the identity of the rate-limiting step in these enzymes, so definitive assignment of the roles of individual amino acids in catalysis based on mutagenesis experiments is not yet possible.

In comparison to AMPK or UMPK, TMPKs contain two fewer arginine residues that can potentially interact with the transferred phosphoryl group. Such an interaction, made by positively charged residues, would act to stabilize the transition state. Notably, of these two arginines in the human TMPK, Arg15 and Arg97, only the latter is seen to interact with the phosphate that would correspond to the γ-phosphate of ATP. One possible explanation for this observation is that *in vivo* an additional factor interacts with human TMPK and can induce the P-loop's arginine to make the above mentioned interaction, and possibly also contributes an additional arginine to the active site. Such a scenario would be similar to the situation in $p21^{ras}$ where GTPase-activating protein (GAP), in addition to assembling the residues at the active site, provides a catalytic residue. This is an attractive possibility because the activity of isolated human TMPK is in fact very low. Thus, such a factor would add another level of control in addition to transcriptional control.

Interpretation of the structures as snapshots along the reaction coordinate

The structures can be pieced together as snapshots in a 'catalytic movie' used to analyze the phosphoryltransfer in the forward reaction and to deduce the dynamics of the reaction. The following is an interpretation of the structures presented pinpointing the likely conformational changes, for both enzyme and nucleotides, that occur during the overall phosphoryltransfer reaction. Making the assumption that human TMPK operates by a bi-bi mechanism to catalyze phosphoryltransfer, as demonstrated for mouse TMPK [9], for AMPK [11] and GMPK [10], we can draw the simple reaction scheme shown in Figure 5a. Our structures of human TMPK, however, suggest that this reaction scheme should be extended by at least two steps in order to account for the different conformations observed.

As we lack structural information on the free and singly bound enzyme, the opening scene is represented by the TMP and AppNHp complex structure (state A Figure 5b). The P-loop and LID have already undergone a conformational change from the open form to the P-loop partially closed state. However, in this state the TMP phosphoryl group is not ideally positioned for nucleophilic attack on the γ-phosphate of ATP. Therefore, we hypothesize that before the chemical step can take place the TMP phosphoryl group swings away from Arg45 towards Arg97 and the phosphate group of ATP, shortening the distance to the donor nucleotide (state B Figure 5b). Arg97 now acts as a clamp to bring the donor and acceptor nucleotides together.

As a model for the transition state of the chemical step, we use the structure of the complex with bound AlF_3. In this state, the oxygen of the TMP phosphoryl group is optimally positioned for attack on the γ-phosphate of ATP. As the phosphoryltransfer takes place, the P-loop and LID adopt the fully closed conformation, and the P-loop Asp15 enhances its interaction with the 3′-hydroxyl of TMP. The TP_5A complex structure is interpreted to represent the enzyme conformation just after the reaction has taken place (state C Figure 5b). This state is probably only observable because of the restraints imposed by using the covalently linked phosphate chain in TP_5A. Without this constraint, the phosphate groups of TDP and the sidechain of Arg97 rotate to the stable product conformation (state D, Figure 5b) represented by the complex with TDP and ADP. As in the TP_5A complex, the enzyme adopts a fully closed conformation.

Biological implications

The structures of various complexes between human thymidylate kinase (TMPK) and nucleotides presented here detail the enzyme and nucleotide conformational changes that occur during catalysis. Despite the limit imposed by the technique of monochromatic X-ray crystallography used in these studies, where only static structures are observed, combining the information from several structures provides valuable information for understanding the dynamics of the reaction.

In the presence of bound nucleotides, the active site of human TMPK adopts a globally closed conformation, as seen earlier for adenylate kinase (AMPK) and uridylate kinase (UMPK). In contrast to these two enzymes, however, further structural changes at the active site appear to be required for catalysis in human TMPK. It seems likely that these processes limit the overall catalysis rate of human TMPK, which in its isolated state is several orders of magnitude less efficient than AMPK, UMPK or even the highly homologous yeast TMPK. Therefore, the question arises as to whether a mechanism or factor is present in the cell for acceleration of this surprisingly slow reaction. This could involve covalent

modification (e.g., phosphorylation) or interaction with a protein factor which favours the catalytically competent structure of the active site, or even supplies further catalytic residues. Such a factor or mechanism would add another level of control to the activity of the protein, in addition to that of cell-cycle-dependent transcriptional control.

Materials and methods

Protein purification and crystallization

Human TMPK (wild type and the Arg200→Ala-mutant) was expressed as a GST fusion protein essentially as described previously [7] and purified to homogeneity by GST affinity chromatography followed by gel filtration. Crystals of human TMPK in complex with nucleotides (TMP and ADP, TMP and AppNHp, TDP and ADP, and the bisubstrate inhibitor TP_5A) were grown by the vapor diffusion method using the hanging-drop geometry. After formation of the respective complex by mixing the nucleotides (end concentrations of: 1 mM TMP and ADP; 1 mM TMP and 20 mM AppNHp; 1 mM TMP and 20 mM ATP; 2 mM TP_5A) and the enzyme solution (28 mg ml^{-1} TMPK, 50 mM $MgCl_2$, 200 mM KCl, 50 mM Tris/HCl pH 8.0), 2 µl of the premixed solution was added to 2 µl of the reservoir solution (15–22 % w/v PEG 3350, 5% v/v of sterile filtered dead sea water, and 100 mM Tris/HCl pH 8.0 and left to equilibrate (at 20°) against the reservoir. Typically, crystals grow within one to two weeks to dimensions of $500 \times 300 \times 300\ \mu m^3$. As cocrystallization with 1 mM AlF_3, 10 mM NaF did not result in additional electron density at the active site, the TMPK complex with TMP, ADP and AlF_3 was prepared by soaking crystals of TMPK containing the nucleotides TMP and ADP overnight in 85 mM $AlCl_3$, 250 mM NaF. This procedure resulted in additional electron density at the active site and a decrease of the high-resolution diffraction to 2.0 Å. The complex of TMPK with TDP and ADP was obtained in the presence of the substrates TMP and

Table 1

Data collection and refinement statistics.

	TMP–ADP	TMP–AppNHp	TMP–ADP–AlF_3	TDP–ADP	TP_5A
X-ray source	NSLS, X25	DESY, BW7B	ESRF, ID14,3	rot. anode	DESY, X11
Wavelength (Å)	1.100	0.847	0.931	1.54	0.9076
Detector	B4-CCD	MAR345	MAR CCD	MAR345	MAR345
Temperature (K)	100	100	100	100	100
Data collection statistics					
Space group	$P4_32_12$	$P4_32_12$	$P4_32_12$	$P4_32_12$	$P4_32_12$
Unit cell (Å)					
a = b	101.0	101.3	101.6	101.1	101.1
c	49.8	49.3	49.3	49.2	49.3
Resolution (Å)	1.63	1.6	1.9	1.7	1.7
Observed reflections	325,999	103,211	106,992	139,922	148,714
Unique reflections	31,064	33,305	20,787	28,445	27,940
Completeness (%)					
Overall/last shell	95.7/75.3	96.6/98.0	99.4/99.5	99.4/99.6	97.4/89.3
R_{sym}* (%)					
Overall/last shell	6.1/20.3	4.6/15.5	7.5/46.3	5.2/29.6	3.3/22.2
Molecules/asymmetric unit	1	1	1	1	1
Refinement statistics					
Resolution range (Å)	33.5–1.65	71.7–1.6	71.8–2.0	50.5–1.7	35.3–1.7
Reflections with $F > 0\sigma$					
Working	27897	29949	16955	25586	25079
Test	3109	3355	930	2859	2772
R_{cryst}† (%)	20.1	19.8	21.4	19.1	19.2
R_{free}‡ (%)	24.2	23.6	27.2	24.0	23.0
No. of protein atoms§	1647	1709	1617	1627	1646
No. of nucleotide atoms§	48	100	48 / 4	73	52
No. of water atoms	293	300	173	277	250
No. of magnesium ions#	3	2	2	2	2
Rms deviations					
bond lengths (Å)	0.012	0.011	0.018	0.012	0.012
bond angles (°)	1.6	1.7	1.6	1.3	1.5
Average B (Å^2)					
mainchain	17.6	21.9	38.8	22.2	24.5
sidechain	21.1	26.4	42.0	26.1	28.2
water molecules	30.7	39.5	51.9	38.3	38.7
nucleotides	16.9	20.1	40.0 / 64.0	19.8	25.0
magnesium ions	22.9	21.0	39.5	22.0	25.0

*$R_{sym} = \Sigma|I_{obs} - \langle I \rangle| / \Sigma \langle I \rangle$. †$R_{cryst} = \Sigma|F_{obs} - F_{calc}| / \Sigma F_{obs}$. ‡$R_{free} = R_{cryst}$, calculated for randomly selected reflections not included in the refinement. §Number includes residues modeled in double conformations and residues modeled as alanine if no electron density for the sidechain is observed; for details see PDB header. In the case of the AlF_3 complex, 48 nucleotide atoms and the four atoms of AlF_3 were modeled. #Only one of the metal ions is bound to ADP/ATP.

ATP in the crystallization solution with a 20-fold excess of ATP over TMP to shift the equilibrium between TMP and TDP towards the product TDP in solution. The idea to crystallize the product complex using the substrates TMP and ATP as starting material arose from observations made when crystallizing TMPK in complex, with TMP and the ATP analog ATPγS (in ATPγS one oxygen atom of the γ-phosphoryl group of ATP is replaced by a sulfur atom). In the latter complex, no electron density for the γ-phosphoryl group of ATPγS was detectable, but instead we observed electron density for a second phosphoryl group on the TMP site (NO *et al.*, unpublished results). We interpret the electron density as TDPβS and ADP.

Data collection and structure determination

X-ray data were collected at 100K from liquid nitrogen flash-cooled crystals using 10% xylitol and 10% glucose as cryoprotectant. The X-ray sources and detectors used for data collection are listed in Table 1. Data were processed with XDS [24] and merged with XSCALE.

The structure of human TMPK was solved by the molecular replacement method with the program AMoRe [25] – thereby also establishing the correct enantiomorph of the space group, which contains one monomer per asymmetric unit – with the yeast TMPK coordinates (all residues modeled as alanine) as search model. Refinement using the rigid-body and simulated annealing protocols as implemented in X-PLOR [26] resulted in a model used to calculate the initial electron-density map, which was of high quality and allowed the unambiguous assignment and building of most sidechains using the program O [27]. Electron density for both nucleotides (TMP and ADP) and the catalytic magnesium ion was observed, but only modeled after most of the protein mainchain and sidechain atoms were built and refined. We noticed that the sidechain of Arg200 (not a conserved residue) from a symmetry-related molecule (not the second monomer of the active dimer) interacts with the β-phosphate of ADP. To avoid this crystal-packing interaction with the nucleotides – which would complicate any interpretation – we mutated Arg200 to alanine. As steady-state analysis of the Arg200→Ala mutant yields identical results to that performed with wild-type TMPK (k_{cat} 0.7 s^{-1}), and as the structures of both constructs in complex with TMP and ADP are identical within the coordinate errors, all subsequent crystallographic experiments were performed with the Arg200→Ala mutant. The final model of the complex of TMPK with TMP and ADP was used as starting model for the refinement of all other complexes reported here. After an initial simulated annealing step (T = 3000K) using X-PLOR [26], the refinement (including individual temperature factors) was carried on with PROTEIN/REFMAC [25]. The occupancies of alternative conformations and of the nucleotides were derived visually using SigmaA-weighted $mF_{obs}–DF_{calc}$ electron-density maps [25]. The refinement statistics are summarized in Table 1.

As the electron-density map of TMPK crystallized in the presence of TMP and AppNHp shows a mixture of ADP and AppNHp bound at the phosphoryl donor-binding site (both modeled with an occupancy of 0.5), we repeated the crystallization using the micro-seeding technique. This procedure reduces the time for crystal growth to two days so that hydrolysis of AppNHp in the crystallization solution is reduced. The crystals were immediately flash cooled and a second data set was collected. The refined structure of this data set also shows a mixture of ADP and AppNHp bound at the phosphoryl donor site with the P-loop and LID in two conformations. However, the occupancy of AppNHp and the corresponding conformations of the P-loop, LID and the phosphoryl group of the monophosphate were determined to be two-thirds. This additional experiment proves that the different conformations of the P-loop, LID and the TMP phosphoryl group correlate with the presence of a diphosphate or triphosphate at the ATP-binding site (see results).

Accession numbers

Coordinates of the human TMPK complex structures and the corresponding structure factors have been deposited in the Protein Data Bank with entry codes 1e2q (TMP–ADP), 1e2f (TMP–AppNp), 1e2e (TMP–ADP–AlF_3), 1e2g (TDP–ADP) and 1e2g (TP_5A).

Supplementary material

Supplementary material including a stereoview of the nucleotides observed in the TMP–ADP–AlF_3 complex and a discussion on the role of Asp15 is available at http://current-biology.com/supmat/supmatin.htm.

Acknowledgements

We thank Sonja Hönig and Georg Holtermann for excellent technical assistance, and Andrew Mesecar for helpful discussions. We thank Michael Weyand for help in data collection. AL and IS acknowledge the generous support by the Peter und Traudl Engelhorn Stiftung, and the Richard and Anne-Liese Gielen-Leyendecker-Stiftung, respectively. Beamline X12C is supported by the US Department of Energy Offices of Health and Environmental Research and of Basic Energy Sciences.

References

1. Jong, A.Y. & Campbell, J.L. (1984). Characterization of *Saccharomyces cerevisiae* thymidylate kinase, the CDC8 gene product. General properties, kinetic analysis, and subcellular localization. *J. Biol. Chem.* **259**, 14394-14398.
2. Su, J.Y. & Sclafani, R.A. (1991). Molecular cloning and expression of the human deoxythymidylate kinase gene in yeast. *Nucleic Acids Res.* **19**, 823-827.
3. Liang, P., Averboukh, L., Zhu, W., Haley, T. & Pardee, A.B. (1995). Molecular characterization of the murine thymidylate kinase gene. *Cell Growth Differ.* **6**, 1333-1338.
4. Lavie, A., Vetter, I.R., Konrad, M., Goody, R.S., Reinstein, J. & Schlichting, I. (1997). Structure of thymidylate kinase reveals the cause behind the limiting step in AZT activation. *Nat. Struct. Biol.* **4**, 601-604.
5. Lavie, A., *et al.* & Schlichting, I. (1998). Structural basis for efficient phosphorylation of 3′-azidothymidine monophosphate by *Escherichia coli* thymidylate kinase. *Proc. Natl Acad. Sci. USA* **95**, 14045-14050.
6. Saraste, M., Sibbald, P.R. & Wittinghofer, A. (1990). The P-loop – a common motif in ATP – and GTP-binding proteins. *Trends Biochem. Sci.* **15**, 430-434.
7. Brundiers, R., *et al.* & Konrad, M. (1999). Modifying human thymidylate kinase to potentiate azidothymidine activation. *J. Biol. Chem.* **274**, 35289-35292.
8. Reynes, J.P., Tiraby, M., Baron, M., Drocourt, D. & Tiraby, G. (1996). *Escherichia coli* thymidylate kinase: molecular cloning, nucleotide sequence, and genetic organization of the corresponding *tmk* locus. *J. Bacteriol.* **178**, 2804-2812.
9. Cheng, Y.C. & Prusoff, W.H. (1973). Mouse ascites sarcoma 180 thymidylate kinase. General properties, kinetic analysis, and inhibition studies. *Biochemistry* **12**, 2612-2619.
10. Li, Y., Zhang, Y. & Yan, H. (1996). Kinetic and thermodynamic characterizations of yeast guanylate kinase. *J. Biol. Chem.* **271**, 28038-28044.
11. Rhoads, D.G. & Lowenstein, J.M. (1968). Initial velocity and equilibrium kinetics of myokinase. *J. Biol. Chem.* **243**, 3963-3972.
12. Vonrhein, C., Schlauderer, G.J. & Schulz, G.E. (1995). Movie of the structural changes during a catalytic cycle of nucleoside monophosphate kinases. *Structure* **3**, 483-490.
13. Abele, U. & Schulz, G.E. (1995). High-resolution structures of adenylate kinase from yeast ligated with inhibitor Ap5A, showing the pathway of phosphoryl transfer. *Protein Sci.* **4**, 1262-1271.
14. Scheffzek, K., Kliche, W., Wiesmüller, L. & Reinstein, J. (1996). Crystal structure of the complex of UMP/CMP kinase from *Dictyostelium discoideum* and the bisubstrate inhibitor P1-(5′-adenosyl) P5-(5′-uridyl) pentaphosphate (UP5A) and Mg^{2+} at 2.2 Å: implications for water-mediated specificity. *Biochemistry* **35**, 9716-9727.
15. Schlichting, I. & Reinstein, J. (1997). Structures of active conformations of UMP kinase from *Dictyostelium discoideum* suggest phosphoryl transfer is associative. *Biochemistry* **36**, 9290-9296.
16. Lavie, A., Konrad, M., Brundiers, R., Goody, R.S., Schlichting, I. & Reinstein, J. (1998). Crystal structure of yeast thymidylate kinase complexed with the bisubstrate inhibitor P1-(5′-adenosyl) P5-(5′-thymidyl) pentaphosphate (TP5A) at 2.0 Å resolution: implications for catalysis and AZT activation. *Biochemistry* **37**, 3677-3686.
17. Berry, M.B., Meador, B., Bilderback, T., Liang, P., Glaser, M. & Phillips, G.N., Jr. (1994). The closed conformation of a highly flexible protein:

the structure of *E. coli* adenylate kinase with bound AMP and AMPPNP. *Proteins* **19**, 183-198.
18. Wittinghofer, A. (1997). Signaling mechanistics: aluminum fluoride for molecule of the year. *Curr. Biol.* **7**, R682-R685.
19. Schlichting, I. & Reinstein, J. (1999). pH influences fluoride coordination number of the AlFx phosphoryl transfer transition state analog. *Nat. Struct. Biol.* **6**, 721-723.
20. Scheidig, A.J., Burmester, C. & Goody, R.S. (1999). The pre-hydrolysis state of $p21^{ras}$ in complex with GTP: new insights into the role of water molecules in the GTP hydrolysis reaction of ras-like proteins. *Structure* **7**, 1311-1324.
21. Smith, C.A. & Rayment, I. (1996). X-ray structure of the magnesium(II)·ADP·vanadate complex of the *Dictyostelium discoideum* myosin motor domain to 1.9 Å resolution. *Biochemistry* **35**, 5404-5417.
22. Müller, C.W. & Schulz, G.E. (1988). Structure of the complex of adenylate kinase from *Escherichia coli* with the inhibitor P1,P5-di(adenosine-5′-)pentaphosphate. *J. Mol. Biol.* **202**, 909-912.
23. Müller, C.W. & Schulz, G.E. (1992). Structure of the complex between adenylate kinase from *Escherichia coli* and the inhibitor Ap5A refined at 1.9 Å resolution. A model for a catalytic transition state. *J. Mol. Biol.* **224**, 159-177.
24. Kabsch, W. (1993). Automatic processing of rotation diffraction data from crystals of initially unknown symmetry and cell constants. *J. Appl. Crystallogr.* **24**, 795-800.
25. Collaborative Computational Project No. 4 (1994). The CCP4 suite: programs for protein crystallography. *Acta Crystallogr. D* **50**, 760-770.
26. Brünger, A.T. (1993) *X-PLOR: a system for X-ray crystallography and NMR*. Yale University Press, New Haven, CT.
27. Jones, T.A., Zhou, J.-Y., Cowan, S.W. & Kjeldgaard, M. (1991). Improved methods for building protein models in electron density maps and the location of errors in these models. *Acta Crystallogr. A* **47**, 110-119.
28. Kraulis, P.J. (1991). MOLSCRIPT: a program to produce both detailed and schematic plots of protein structures. *J. Appl. Crystallogr.* **24**, 946-950.
29. Merrit, E.A. & Murphy, M.E.P. (1994). Raster3D Version 2.0 – a program for photorealistic molecular graphics. *Acta. Crystallogr. D* **50**, 869-873.